Cellular Signalling 59 (2019) 62–75

Contents lists available at ScienceDirect

Cellular Signalling

journal homepage: www.elsevier.com/locate/cellsig

Panobinostat (LBH589) inhibits Wnt/β-catenin signaling pathway *via* upregulating APCL expression in breast cancer

Ge Qin[a,1], Yizhuo Li[a,1], Xiangdong Xu[b,1], Xin Wang[a], Kai Zhang[a], Yanlai Tang[c], Huijuan Qiu[a], Dingbo Shi[a], Changlin Zhang[a], Qian Long[a], Kaping Lee[a], Qinglian Zhai[a], Shusen Wang[a], Miao Chen[a,*], Wuguo Deng[a,*]

[a] State Key Laboratory of Oncology in South China, Collaborative Innovation Center of Cancer Medicine, Sun Yat-sen University Cancer Center, Guangzhou, China
[b] Department of Thyroid & Breast Surgery, The First Affiliated Hospital, Sun Yat-sen University, Guangzhou, China
[c] Department of Pediatrics, The First Affiliated Hospital, Sun Yat-sen University, Guangzhou, China

ARTICLE INFO

Keywords:
Panobinostat
APCL
Wnt/β-catenin signaling pathway
Breast cancer

ABSTRACT

Breast cancer is the most common malignant disease among women worldwide and the novel therapeutic agents are urgently needed. Panobinostat (LBH589), a pan-HDACs inhibitor, has shown promising anti-tumor effect in recent years. However, the targets of this compound are largely unclear because of its low selectivity. In consideration of the transcription promoting activity of panobinostat, we speculated that specific tumor suppressor genes might be upregulated after panobinostat treatment. In this study, we verified the inhibition effect of panobinostat in different subtypes of breast cancer cells *in vivo* and *in vitro*. We found that panobinostat suppressed proliferation, migration as well as invasion, and induced apoptosis in both TNBC and non-TNBC cells. Consistently, panobinostat inhibited breast cancer growth and metastasis in mouse models. Mechanistically, we found APCL transcription and expression was significantly upregulated in panobinostat treated cells by RNA microarray analysis, while knockdown of APCL resulted in reduced sensitivity to panobinostat in breast cancer cells. APCL is a wnt/β-catenin pathway regulator that promotes β-catenin ubiquitylation and degradation. We found that panobinostat inhibited β-catenin expression by increasing its ubiquitylation and thus reducing its half-life. In addition, the expression of β-catenin activated targets including c-Jun, c-Myc, Cyclin D1 and CD44 were also decreased by panobinostat treatment in breast cancer cells. These results suggested that panobinostat inhibited tumor growth and metastasis *via* upregulating APCL expression in breast cancer cells, which was a novel and crucial mechanism of panobinostat.

1. Introduction

Breast cancer is the most common malignant disease among women worldwide, which leads to approximately 15% of cancer death in women [1]. Breast cancer is a heterogeneous disease and is characterized by hormone receptor expression, HER-2 expression and ki67 status. Though endocrine therapy and anti-HER-2 therapy have dramatically increased the overall survival of breast cancer, tumor recurrence, metastasis and drug tolerance are enormous challenges for breast cancer management. The explorations for new drugs and therapeutic targets are eagerly needed.

The role of epigenetic modifications in tumorigenesis and progression has raised great interest these years. Chromatin is the high-order structure of DNA and proteins, which is a barrier for gene transcription. Nucleosomes, the basic unit of chromatin, consist of four kinds of histones, H2A, H2B, H3 and H4 [2]. The functions of histones are regulated by multiple post-translational modifications, such as reversible acetylation of the amino-terminal ε-group of lysines on histones. The acetylation of histone leads to a looser chromatin structure, which enables better accessibility to the transcription machinery [3,4]. The balance of histone acetylation is regulated by histone acetyltransferases (HATs) and histone deacetylases (HDACs) [5]. Until now, 18 HDACs

* Corresponding authors at: Sun Yat-Sen University Cancer Center, 651 Dongfeng East Road, Guangzhou 510060, China.
E-mail addresses: qinge@sysucc.org.cn (G. Qin), liyzh@sysucc.org.cn (Y. Li), wangxin1@sysucc.org.cn (X. Wang), zhangkai@sysucc.org.cn (K. Zhang), tangylai@mail.sysu.edu.cn (Y. Tang), qiuhj@sysucc.org.cn (H. Qiu), shidb@sysucc.org.cn (D. Shi), zhangchl@sysucc.org.cn (C. Zhang), longqian@sysucc.org.cn (Q. Long), lijiap@sysucc.org.cn (K. Lee), zhaiql@sysucc.org.cn (Q. Zhai), wangshs@sysucc.org.cn (S. Wang), chenmiao@sysucc.org.cn (M. Chen), dengwg@sysucc.org.cn (W. Deng).
[1] These authors contributed equally to this article.

https://doi.org/10.1016/j.cellsig.2019.03.014
Received 31 December 2018; Received in revised form 12 March 2019; Accepted 13 March 2019
Available online 14 March 2019
0898-6568/

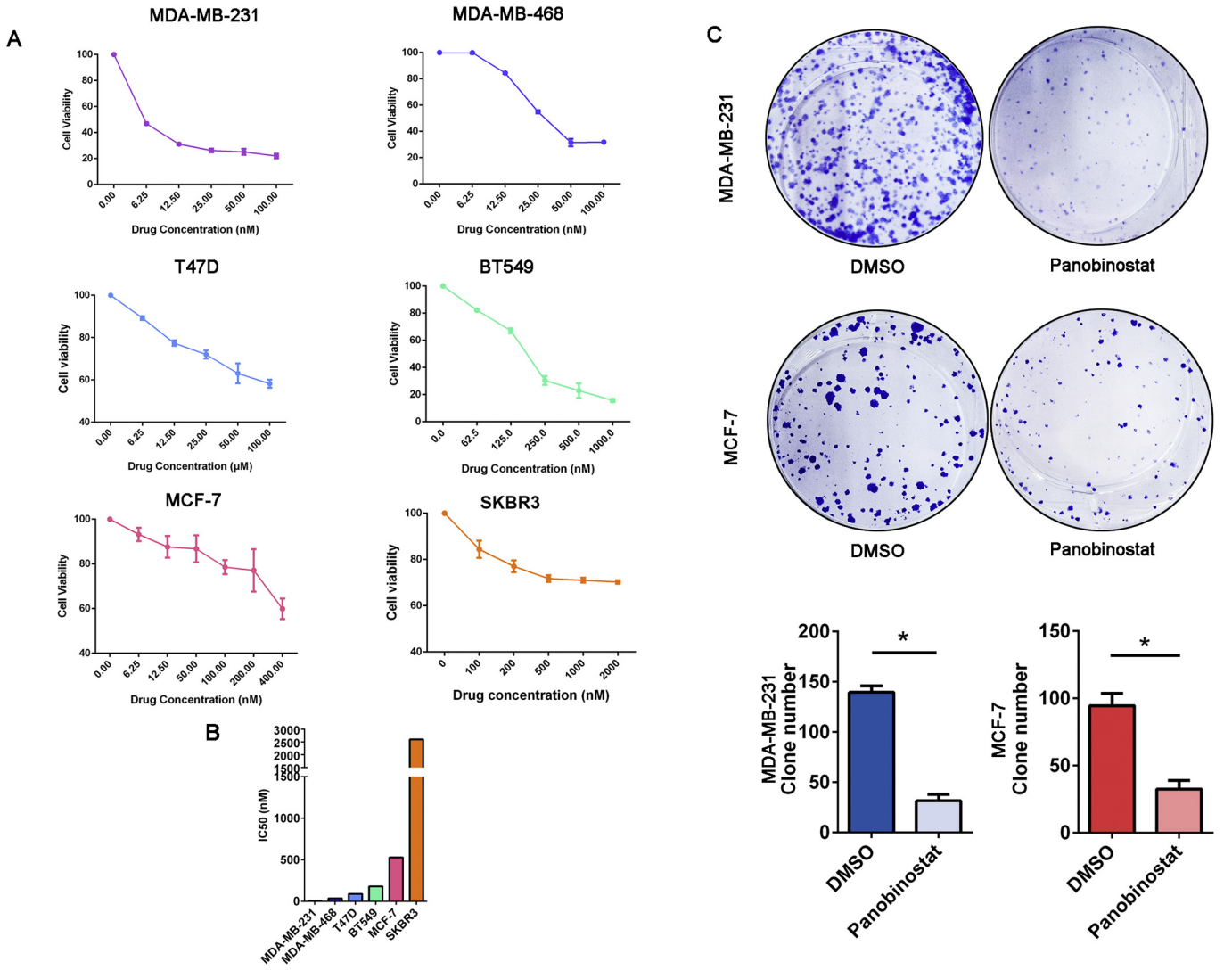

Fig. 1. Panobinostat inhibited breast cancer cell proliferation. (A) MTS assay was performed in different breast cancer cells treated with different doses of panobinostat. MDA-MB-231, MDA-MB-468 and BT549 are triple-negative breast cancer cell lines, T47D and MCF-7 are luminal subtype breast cancer cell lines with ER positive expression and SKBR3 is a HER-2 amplified cell line. (B) IC50 of panobinostat for the six breast cancer cell lines was presented by bar graph. (C) Plate clone formation assay was conducted with MDA-MB-231 and MCF-7 cells treated with 0.5 μM panobinostat. The clone numbers were counted and shown with histograms. Data were presented as mean ± s.d. of three independent experiments, and the significance of difference between groups was analyzed by Student's *t*-test. $^{*}P < .05$.

has been identified and grouped into four classes [6]. As histone acetylation level is significantly related to gene expression, it has been reported to be associated with cancer development. A low level of histone H3 lysine 18 acetylation (H3K18ac) was found to predict poor survival in pancreatic, prostate, lung and breast cancers. In addition, it was also reported that low level of histone H4 lysine 16 monoacetylation (H4K16ac) was an early event in breast cancer development [7]. Suziki et al. found reduced acetylated H4 in ductal carcinoma in breast cancer when compared with the normal breast epithelium [8]. Therefore, the compounds targeting HDACs are considered as a promising therapeutic approach for human cancers including breast cancer.

Panobinostat (LBH589) is one of the novel pan-HDAC inhibitors, and has demonstrated promising activity as an antitumor small molecular compound [9]. In breast cancer, one study showed that panobinostat treatment restored ER expression in ER negative breast cancer cell lines MDA-MB-231 and MDA-MB-435, and panobinostat was considered to have synergistic effect with endocrine therapies [10]. Also, Kubo et al. reported that panobinostat increased the sensibility to aromatase inhibitors of breast cancer cells that were originally resistant to aromatase inhibitors [11]. Moreover, the anti-tumor effect of panobinostat has been observed in triple negative breast cancers (TNBCs). Tate et al. revealed that panobinostat inhibited the proliferation of TNBC cells and decreased the volumes of TNBC xenografts in mice [12]. In addition, another study indicated that panobinostat suppressed the expression of the ZEB family of zinc finger transcription factors, which induced epithelial to mesenchymal transition (EMT) [13]. Though the anti-tumor effect of panobinostat has been explored, the underlying molecular mechanism is still unclear. The targets of this compound need further clarification due to its low selectivity. Considering the transcription promoting activity of panobinostat, we speculated that specific tumor suppressor genes could be upregulated by panobinostat treatment, contributing to its anti-tumor activity.

APCL (also known as APC2) was first isolated in 1998 as a tumor suppressor gene with significant homology to the adenomatous polyposis coli (APC) protein [14]. This gene is located on choromosome 19p13.3 and encodes a 2303 amino-acid protein that is mainly expressed in the brain tissue. Similar to APC, APCL is able to bind to β-catenin and leads its degradation through the ubiquitin-proteasome pathway [15]. Although APCL is less active than APC, it is considered as a crucial tumor suppressor regulating the Wnt/β-catenin signaling

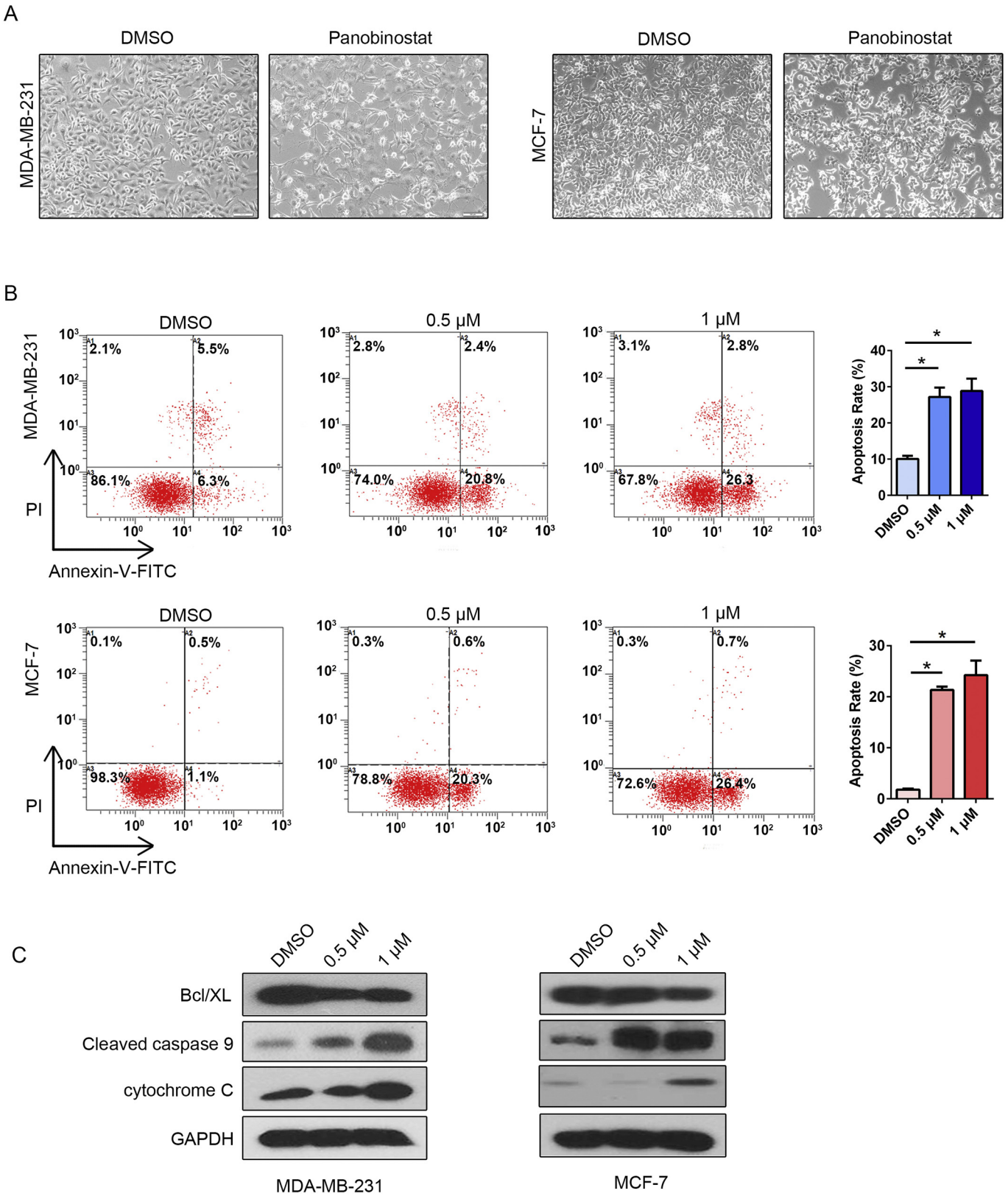

Fig. 2. Panobinostat induced breast cancer cell apoptosis. (A) The cell morphology under microscope with 0 μM and 0.5 μM panobinostat treatment. (B) Cells were treated with 0 μM, 0.5 μM and 1 μM panobinostat for 24 h and apoptosis was detected by flow cytometry. The percentages of apoptotic cells were shown with histograms. Data were presented as mean ± s.d. of three independent experiments, and the significance of difference between groups was analyzed by Student's *t*-test. $^{*}P < .05$.

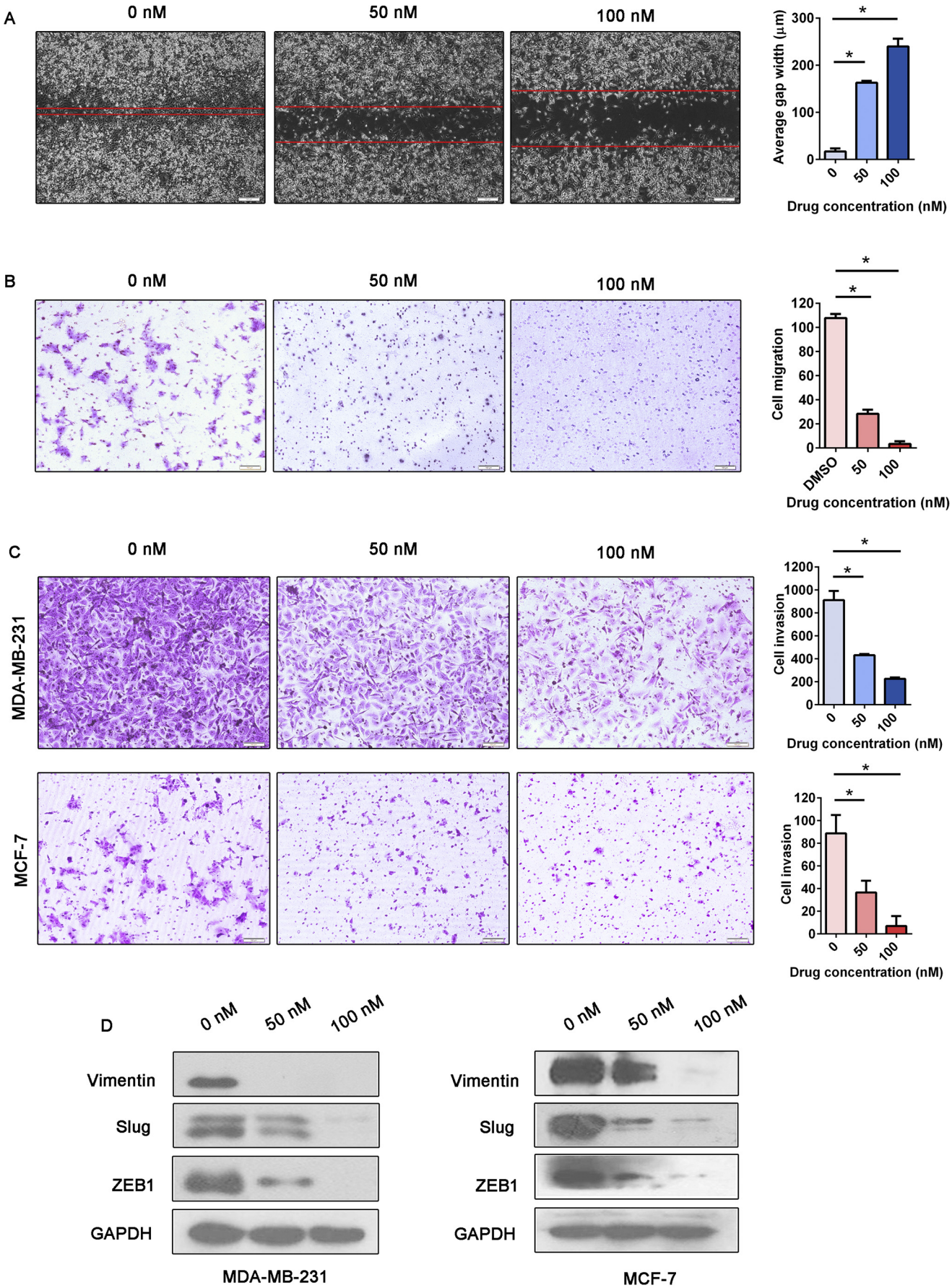

(caption on next page)

Fig. 3. Panobinostat suppressed breast cancer cell migration and invision. (A) Scrach assay was performed in MDA-MB-231 cells treated with 0 nM, 50 nM and 1 nM panobinostat treatment for 48 h. (B) For the migration assay, MCF-7 cells were treated with 0 nM, 50 nM and 100 nM panobinostat for 24 h, then added to the upper compartment of the transwell units without matrigel, and cultured for another 18 h. (C) Invision assay was conducted in MDA-MB-231 and MCF-7 cells. Cells were treated with 0 nM, 50 nM and 100 nM panobinostat for 24 h, then added to the upper compartment of the transwell units with matrigel, and cultured for another 18 h. (D) Westen blot analysis for Vimentin, Slug, and ZEB1. Data were presented as mean ± s.d. of three independent experiments, and the significance of difference between groups was analyzed by Student's *t*-test. $^{*}P < .05$.

pathway [16].

In this study, we first demonstrated the anti-tumor effect of panobinostat in both TNBC and non-TNBC cells *in vitro* and *in vivo*. Next, RNA microarray revealed that APCL expression was significantly up-regulated by panobinostat treatment. Furthermore, we showed that the stability of β-catenin was decreased by panobinostat-induced APCL expression. In addition, the expression of β-catenin target genes were also down-regulated in panobinostat-treated cells. In summary, we propose that APCL is a target of panobinostat and mediates the therapeutic effect of panobinostat in breast cancer cells.

2. Methods

2.1. Cell culture and chemicals

MDA-MB-231, MCF-7, BT549, MDA-MB-468, T47D, SKBR3 and 293FT cells were obtained from American Type Culture Collection (ATCC, Manassas, VA, USA). MDA-MB-231 and 293FT cells were grown in DMEM (Invitrogen, Carlsbad, CA, USA) and MCF-7, BT549, T47D cells were grown in RAPI 1640 (Invitrogen) supplemented with 10% fetal bovine serum (Invitrogen), 100 U/mL penicillin and 100 μg/mL streptomycin (Invitrogen). MDA-MB-468 cell was grown in L-15 medium (Invitrogen) with 10 μg/ml insulin (Sigma, Darmstadt, Germany),16 μg/ml glutathione (Sigma), and supplemented with 10% fetal bovine serum (Invitrogen), 100 U/mL penicillin and 100 μg/mL streptomycin (Invitrogen). All cells were cultured in a humidified atmosphere of 5% CO_2 at 37 °C. Panobinostat (LBH589) was a gift from Novartis (Basel, Swizerland). Panobinostat was prepared in dimethyl sulfoxide (DMSO) as a 50 mM solution, and the stock solution was stored at −20 °C before use.

2.2. Western blot analysis

MDA-MB-231 and MCF-7 cells were seeded in 6-well plates for 48 h with different concentrations of Panobinostat (0 nM, 50 nM, 100 nM, 0.5 μM and 1 μM). A total of 100 μl of RIPA lysis buffer supplemented with 1% protease Inhibitor (Selleck, Houston, TX, USA) was used to lyse cells. Approximately 40–80 μg total protein of each sample was separated by electrophoresis and then transferred to a PVDF membrane (Amersham Biosciences, Piscataway, NJ, USA). Antibodies used for western blot were as follows: APCL (PA5-20944, Invitrogen, 1:500), β-catenin (8480, Cell Signaling Technology, Danvers, MA, USA, 1:1000), c-Jun (9156, Cell Signaling Technology, 1:1000), c-Myc (5605, Cell Signaling Technology, 1:1000), Cyclin D1 (2978, Cell Signaling Technology, 1:1000), acetyl-histone H2A (ET106-34, Huabio, Hangzhou, CHN, 1:1000), acetyl-histone H2B (ET1611-48, Huabio, 1:1000), acetyl-histone H3 (ET1608-9, Huabio, 1:1000), acetyl-histone H4 (ET1602-40, Huabio, 1:1000), GAPDH (10494-1-AP, Proteintech, Rosemont, IL, USA,1:1000), histone H3 (17168-1-AP , Protentech, 1:1000), anti-rabbit secondary antibody (W4011, Promega Corporation, WI, USA, 1:20,000), anti-mouse secondary antibody (W4021, Promega Corporation, 1:10,000). To detect the protein bands, we used the SuperSignal Chemiluminescent Substrates from Thermo Fisher Scientific (31206, Carlsbad, CA, USA). The signal was detected by film and grayscale was measured by Image J.

2.3. MTS assay

MDA-MB-231, MCF-7, BT549, MDA-MB-468, T47D and SKBR3 cells were trypsinized and counted under microscope. 5×10^3 cells/well were added to 96-well culture plates. After the cells attached, panobinostat in indicated concentrations were added in for 48 h. Next, MTS regent [3-(4,5-dimethylthiazol-2-yl)-5-(3-carboxymethoxyphenyl)-2-(4-sulfophenyl)-2H-tetrazolium] (Promega) was diluted with medium to a 20% concentration and added to the cells and culture in 37 °C for 1 h. The optical density (OD) was measured by microplate reader with a 490 nm wavelength.

2.4. Colony formation assay

MDA-MB-231 and MCF-7 cells were seeded in 6-well culture plates and treated with 0 μM and 0.5 μM panobinostat for 48 h. Cells were then harvested and counted under microscope. 400 cells/well were added in 2 ml medium in 6-well culture plates and cultured for 10 days. Next, cells were fixed by 4% paraformaldehyde for 15 min and stained by crystal violet for 15 min. After staining, cells were photographed and counted manually.

2.5. Annexin V/PI apoptosis assay

MDA-MB-231 and MCF-7 cells were seeded in 6-well culture plates and treated with 0 μM,0.5 μM or 1 μM panobinostat for 48 h. Cells were then trypsinized and washed with cold PBS for 3 times. Annexin V-FITC/PI apoptosis kit (KGA108-1, KeyGene Biotech, Jiangsu, CHN) were used in this study according to the manufacturers' instruction.

2.6. Scratch assay

Cells were seeded a 6-well culture plates and incubated overnight to a density of 60%–70%. Cell monolayers were then scratched with a 100-μl pipette tip and washed with PBS three times to remove detached cells. The wounded gaps were imaged using an Olympus microscope and marked. The indicated doses of panobinostat were applied to culture cells for 48 h at 37 °C in 5% CO_2. Afterward, the culture medium was removed, and the same regions were imaged again to observe the wound gap.

2.7. Cell migration and invasion assay

The cell migration and invasion assays were conducted using BD PET-track-etched membrane invasion chamber with (for invasion assay) or without (for migration assay) 20 μl of diluted Matrigel (356234, BD Biosciences, San Jose, CA, USA). The cells were pretreated with 0 nM, 50 nM or 100 nM panobinostat for 24 h. Then, 4×10^4 MDA-MB-231 cells or 6×10^4 MCF-7 cells were added to the upper chamber without FBS. The lower chamber was filled with 1 ml of DMEM with 20% FBS. The chambers were incubated in 37 °C for 18 h, and the invaded cells were stained with crystal violet. The cells that adhered to the membranes were imaged and counted manually.

2.8. RNA microarray analysis

MCF-7 cells were seeded in 10-cm dish and cultured to 80%–90% cell density. After treated with 0 μM or 0.5 μM panobinostat for 24 h,

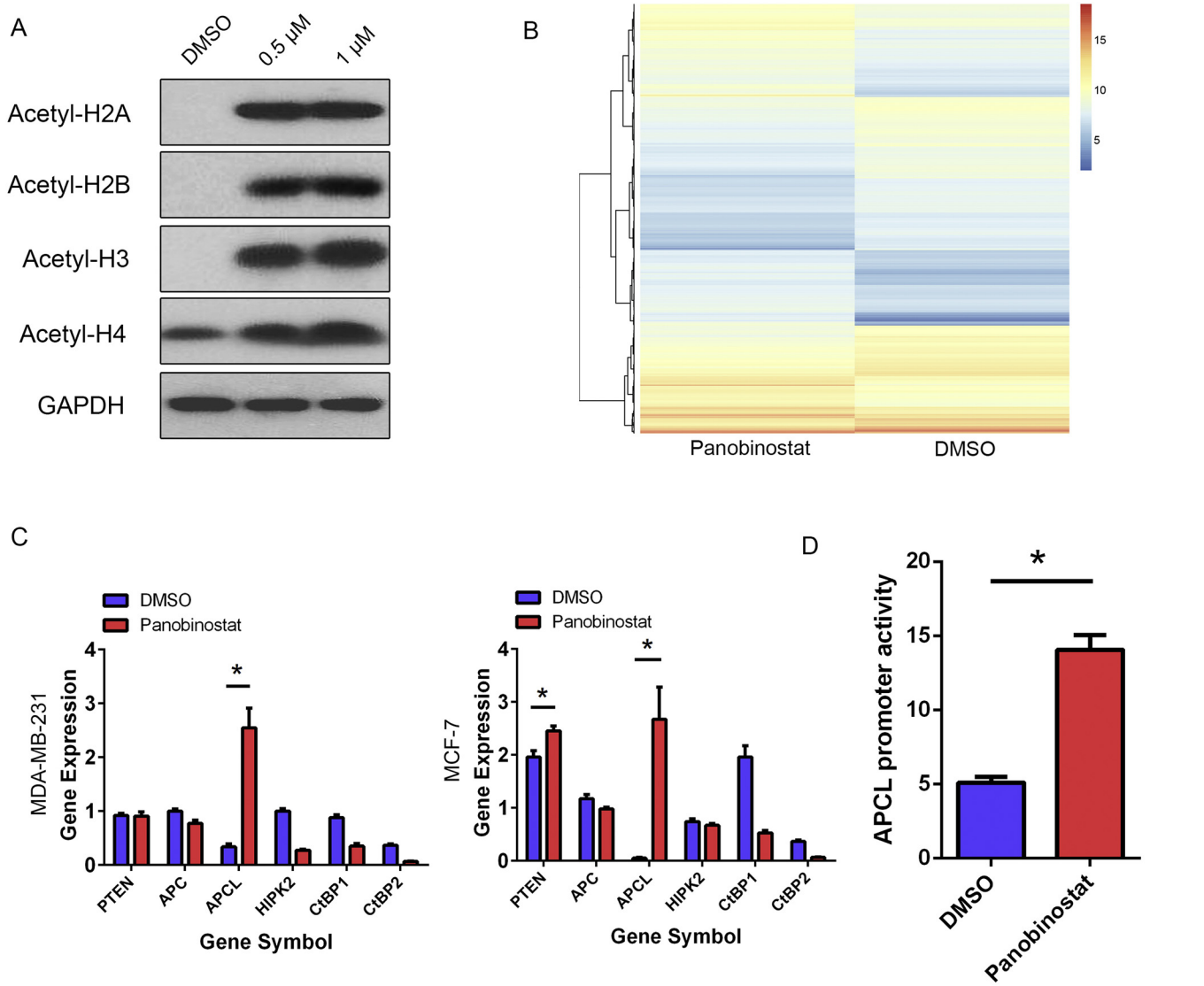

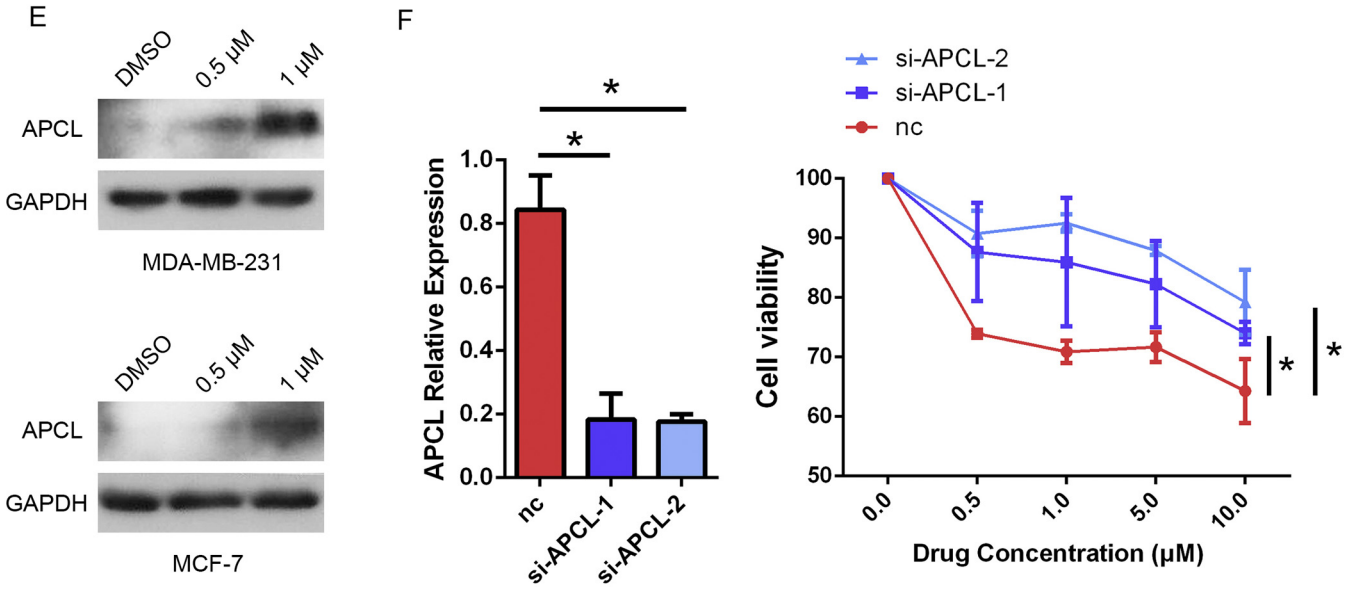

(caption on next page)

Fig. 4. Panobinostat exerted the anti-tumor effect by upregulating the transcritpion of the tumor suppressor gene APCL. (A) Western blot analysis for H2A, H2B,H3 and H4 acetylation. (B) The heat map of RNA micro array analysis in MCF-7 cells treated with 0 μM and 0.5 μM panobinostat for 24 h. (C) The expression of changed genes was further verified by RT-qPCR assay in MDA-MB-231 and MCF-7 cells. (D) Dual-luciferase reporter assay in MDA-MB-231 cells with 0 μM and 0.5 μM panobinostat treatment. (E) Western blot analysis for APCL expression. (F) The expression of APCL was knocked down by si-RNA in MDA-MB-231 cells (left), and the cell viability was measured by MTS assay (right). Data were presented as mean ± s.d. of three independent experiments, and the significance of difference between groups was analyzed by Student's *t*-test. $^{*}P < .05$.

the cells were lysed with 1 ml Trizol (T9424, Sigma Aldrich, St. Louis, MO, USA) and store at −80 °C. RNA microarray analysis was conducted by Shanghai Biotechnology Corporation using Agilent human 4 × 44 k array.

2.9. Real-time fluorescent quantitative PCR assay

MDA-MB-231 and MCF-7 cells were seeded in 6-well plate and treated with panobinostat or si-RNA. After 24 h, the cell total RNA was extracted using RaPure Total RNA Kit (R4001, Magen, GD, China). Then cDNA was synthesized by Reverse Transcription PCR using HiScript Q RT SuperMix for qPCR Kit (R122–01, Vazyme, JS, China). Finally, the expression of target genes were analyzed by qPCR using ChamQ Universal SYBR qPCR Master Mix (Q711–02, Vazyme). The primers used for qPCR assay were listed below: APCL (forward 5′-GGACCGGGAACGGTGTTTC-3′, reverse 5′-AGCTGAGAG- TAGTACC AGAGC-3′); APC (forward 5′-AAAATGTCCCTCCGTTCTTATGG-3′, reverse 5′-CTGAAGTTGAGCGTAATACCAGT-3′); PTEN (forward 5′-AGGGA- CGAACTGGTGTAATGA-3′, reverse 5′-CTGGTCCTTACTTCCC CATAGAA-3′); HIPK2 (forward 5′-AATAGAGCCGAGTTCCAACTGG-3′, reverse 5′-GTCTGC- -TCGTAAGGTAGGCTT-3′); CTBP1 (forward 5′-AAAGCCCTCCGCATCATCG-.

-3′, reverse 5′-AGACGGCAATGCCTAAATCCC-3′); CTBP2 (forward 5′-GAAT- -TGCCGTGTGCAACATCC-3′, reverse 5′-CGTGTTCCTCCGGT ACAGG-3′).

2.10. Survival analysis in Kaplan-Meier plotter database

The survival analysis of APCL in breast cancer was conducted in Kaplan-Meier Plotter database (http://kmplot.com/analysis). The probe number was 205320-at and patients were split by median. Kaplan-Meier analysis was processed in different breast cancer subtypes individually.

2.11. Co-immunoprecipitation (co-IP)

For co-IP, MDA-MB-231 cells were treated with 0 μM or 0.5 μM panobinostat for 24 h before proteasome inhibitor MG-132 was added. 8 h later, cells were lysed and the supernatants were incubated with Protein A/G agarose beads (sc-2003, Santa Cruz, CA, USA, 20 μl) with anti-β-catenin antibody (8480, Cell Signaling Technology, 4 μl) overnight in 4 °C, and the precipitates were washed five times with RIPA and analyzed by western blot. The ubiquitin antibody was obtained from Cell Signaling Technology (3936, 1:1000).

2.12. Dual luciferase reporter assay

MDA-MB-231 cells were seeded in 24-well plates and transfected with 0.5 μg/well luciferase reporter plasmids. To normalize the transfection efficiency, the cells were co-transfected with 10 ng of pRL-CMV (Renilla luciferase). 48 h after transfection, the luciferase activity was detected using Dual-Luciferase Reporter Assay System Kit (E1910; Promega, Madison, WI, USA) according to the manufacturer's instruction. For Top Flash/FOP Flash assay, the reporter plasmid was obtained from Addgene (Watertown, MA, USA).

2.13. Flow cytometry assay

MDA-MB-231 cells were seeded in 6-well culture plates and treated with 0 μM or 0.5 μM panobinostat for 48 h. Cells were trypsinized and washed by PBS for 3 times. Cells were then resuspended by 100 μl PBS and 5 μl FITC-CD44 antibody (11-0441-81, eBioscience, Carlsbad, CA, USA) and isotype antibody (11-4031-82, eBioscience) were added. After culturing for 20 min on ice, cells were centrifuged and re-suspended in 400 μl PBS and detected by cytoFLEX.

2.14. Stable transfection of luciferase

pMX-Luc2 plasmid was transfected into 293FT cells, and the supernatant was collected after 48 h. The luciferase over-expressing lentivirus was isolated from the supernatant. MDA-MB-231 cells were cultured in 6-well culture plates until the cell density reached approximately 40%–50%. The cells were washed with PBS, and 2 ml of DMEM without FBS was added to each well. A 100-μl suspension of the virus with 5 μg/ml polybrene was used to infect the MDA-MB-231 cells. At 72 h after infection, the cells were selected with 1.0 μg/ml puromycin, and the selection was repeated twice. The expression level of luciferase in MDA-MB-231 cells was evaluated by Promega GloMax® 20/20 Fluorescent Module.

2.15. Animals and treatment

Female nude mice aged 4–5 weeks were purchased from Guangdong Laboratory Animal Center and quarantined for 1 week before use. Animal care and experiments involved in this study followed the Accreditation of Laboratory Animal Care International guidelines. Animals and protocols were approved by the guidelines established by the Animal Care Committee at Sun Yat-sen University.

MDA-MB-231-LUC cells were suspended in 100 μl of normal saline. For subcutaneous injection, 2×10^6 cells were injected, and for the metastasis model, 5×10^5 cells were injected through the tail vein. One week after the injection, the animals were randomly divided into two groups and treated as follows: the treatment group, panobinostat at 20 mg/kg [17,18] *via* intraperitoneal injection three times a week; the control group, vehicle (2% DMSO +48% PEG 300 + 2% Tween 80 + ddH2O) at the same time. The weights of the mice in each group were measured weekly.

2.16. Bioluminescence imaging

IVIS Lumina III *in-vivo* imaging system was used to observe the fluorescence signal in mice. The mice were injected with 2 mg luciferin (p1043, promega) and sedated by isoflurane-inhaled anesthesia for 10 min before imaging. The luminescence exposure time was 2 min.

2.17. Histopathology

The HE staining, immunohistochemical staining (IHC) and histopathology analysis were supported by Sun Yat-sen University Cancer Center Pathology Department. The concentration of primary antibody was 1:400 for β-catenin and 1:200 for APCL. The integrated optical density (IOD) value of IHC was measured by Image J Pro Plus 6.0. The photographs of IHC were transformed to a intensity form and the staining area was selected. Then IOD value was measured according to

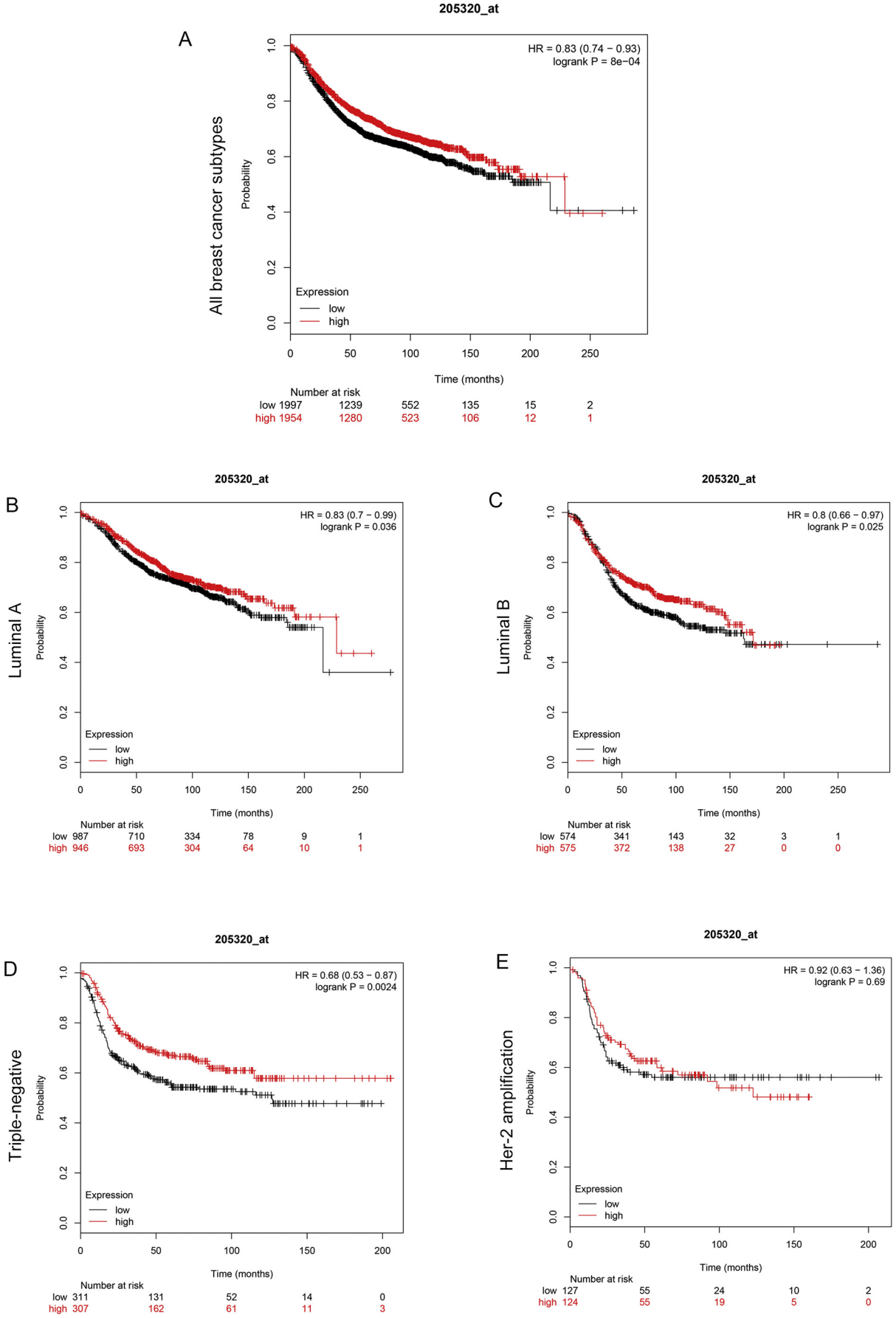

(caption on next page)

Fig. 5. The prognostic value of APCL in breast cancer patients. Kaplan-Meier analysis of APCL in breast cancer patients with different subtypes: (A) The whole cohort including all breast cancer subtypes. (B) Luminal A breast cancer patients. (C) Luminal B breast cancer patients. (D) Triple negative breast cancer patients. (E) HER-2 amplified breast cancer patients.

the staining color and staining area.

2.18. Data analyses

Experimental data and statistic graphs were analyzed using GraphPad Prism 6.0. Student's *t*-test was used to compare the differences between control and treated groups. The mean ± s.d. is presented in all graphs, and significance was defined as $P < .05$. Survival analysis was conducted in Kaplan-Meier Plotter database using Kaplan-Meier curve, and significance was defined as $P < .05$.

3. Results

3.1. Panobinostat inhibited breast cancer cell proliferation

MTS assay [3-(4,5-dimethylthiazol-2-yl)-5-(3-carboxymethoxyphenyl)-2-(4-sulfophenyl)-2H-tetrazolium] was performed to evaluate the cell viability inhibition effect of panobinostat in five different breast cancer cell lines, including triple-negative breast cancer cells (MDA-MB-231, MDA-MB-468 and BT-549), luminal A subtype cells (MCF-7 and T47D), as well as HER-2 amplified cell line SKBR3. We found that 48-hour treatment with panobinostat significantly suppressed the viability of all breast cancer cell lines in a concentration dependent manner (Fig. 1A). Subsequently, the half maximal inhibitory concentrations (IC50) of panobinostat in the six cell lines were analyzed, and MDA-MB-231 was the most sensitive while SKBR3 showed resistance to panobinostat with a dramatically higher IC50 (Fig. 1B). Nonetheless, our results showed that panobinostat had potent inhibitory effect on cell viability in both TNBC and non-TNBC breast cancer cells.

Next, plate clone formation assay was conducted in MDA-MB-231 and MCF-7 cells, and panobinostat treatment (0.5 μM) inhibited the formation of clones in MDA-MB-231 and MCF-7 cells (Fig. 1C). These results suggested that panobinostat suppressed the proliferation of both TNBC and non-TNBC breast cancer cells.

3.2. Panobinostat induced apoptosis in breast cancer cells

We noticed that the morphology of MDA-MB-231 and MCF-7 cells were dramatically changed with 1 μM panobinostat treatment (Fig. 2A), and we inferred that panobinostat might induce apoptosis in breast cancer cells. MDA-MB-231 and MCF-7 cells were treated with ponobinostat in the indicated concentrations for 24 h, and Annexin V/PI was applied to detect apoptotic cells. Fluorescence-activated cell sorting (FACS) analysis showed that panobinostat treatment led to increased apoptosis in breast cancer cells in a concentration dependent manner (Fig. 2B). In addition, western blot was performed to examine the expression of apoptosis markers, and BCL/XL was down-regulated by panobinostat treatment. Consistently, cleaved casepase 9 and cytochrome C were also increased in panobinostat-treated cells (Fig. 2C). These results indicated that panobinostat promoted the apoptosis of breast cancer cells.

3.3. Panobinostat suppressed breast cancer cell mobility and invasion

To evaluate the effect of panobinostat on wound healing ability, we carried out the scratch assay. Panobinostat was used at 50 nM and 100 nM, and 48 h later, the wound healing ability of MDA-MB-231 cells was inhibited in a concentration-dependent manner (Fig. 3A). As MCF-7 cells grew in clumps, it was difficult to conduct the scrach assay. Therefore, transwell assay was performed to investigate the migration ability of MCF-7 cells, which were seeded in the upper compartment without matrigel. After 18 h of culture, the result showed that panobinostat decreased the number of migrated cells (Fig. 3B).

We next analyzed the effect of panobinostat on invasion. Matrigel was added to the upper compartments of the transwell chambers to mimic the extracellular matrix. 18 h later, panobinostat was shown to inhibit the invasion of both MDA-MB-231 and MCF-7 cells in a dose-dependent manner. The number of invading cells in the high-concentration group was significantly decreased than that of untreated group (Fig. 3C).

Vimentin, Slug and ZEB1 are crucial molecules involved in EMT progression and have a vital role in breast cancer cell migration and invasion. We therefore analyzed the effects of panobinostat on the expression of these EMT markers by western blot. As expected, the drug-treated cells had lower expression of vimentin, Slug and ZEB1, especially at the higher concentration of 100 nM (Fig. 3D).

3.4. Panobinostat exerted the anti-tumor effect by upregulating APCL transcription

Panobinostat is a pan-HDAC inhibitor, and we found that this compound increased the acetylation level of the four histones that consist of the nucleosomes (Fig. 4A). We speculated that the transcription of some tumor suppressor genes could be promoted by panobinostat. Therefore, RNA microarray was conducted to identify the variable genes (Fig. 4B). Among these genes, PTEN, APC, APCL, HIPK2, CtBP1 and CtBP2 were selected as candidates for they were reported to have tumor suppressing function. RT-qPCR was conducted to further confirm the gene expression changes, and we found that the expression of APCL dramatically increased in both MDA-MB-231 and MCF-7 cells treated with 0.5 μM panobinostat for 24 h (Fig. 4C). Consistently, APCL expression of BT549 and T47D cells were also significantly upregulated after 0.5 μM panobinostat treated for 24 h (Fig. S1A). Moreover, dual-luciferase reporter assay showed that APCL promoter activity was upregulated by 0.5 μM panobinostat treatment (Fig. 4D), and the protein level of APCL was also increased by panobinostat at indicated concentrations (Fig. 4E). In contrast, when APCL was knocked down in MDA-MB-231 cells by small interfering RNA (si-RNA), panobinostat became less effective in suppressing the viability of the cells (Fig. 4F). These results suggested that APCL was a crucial target of panobinostat.

3.5. Low APCL expression predicted poor prognosis in breast cancer

As APCL is reported as a tumor suppressor gene, we further analyzed its prognostic value using the Kaplan-Meier plotter database [19]. The survival analysis for all breast cancer subtypes was shown in Fig. 5A. We found that patients with low APCL expression had poorer outcomes. We next conducted the subgroup analysis, for breast cancer had high heterogeneity between different subtypes. The result demonstrated that APCL high expression is a favorable prognostic factor in Luminal A, Luminal B, and especially triple-negative breast cancer patients (Fig. 5B, C and D). However, there was no statistic significance in HER-2 amplified breast cancer (Fig. 5E).

3.6. Panobinostat reduced β-catenin stability and inhibited the wnt/β-catenin pathway by inducing APCL expression

APCL is known to be a wnt/β-catenin pathway regulator like APC. APCL is a component of the β-catenin degration complex and promotes β-catenin dagration by ubiquitination. Therefore, we further explored the activity of the wnt/β-catenin pathway. Western blot showed that

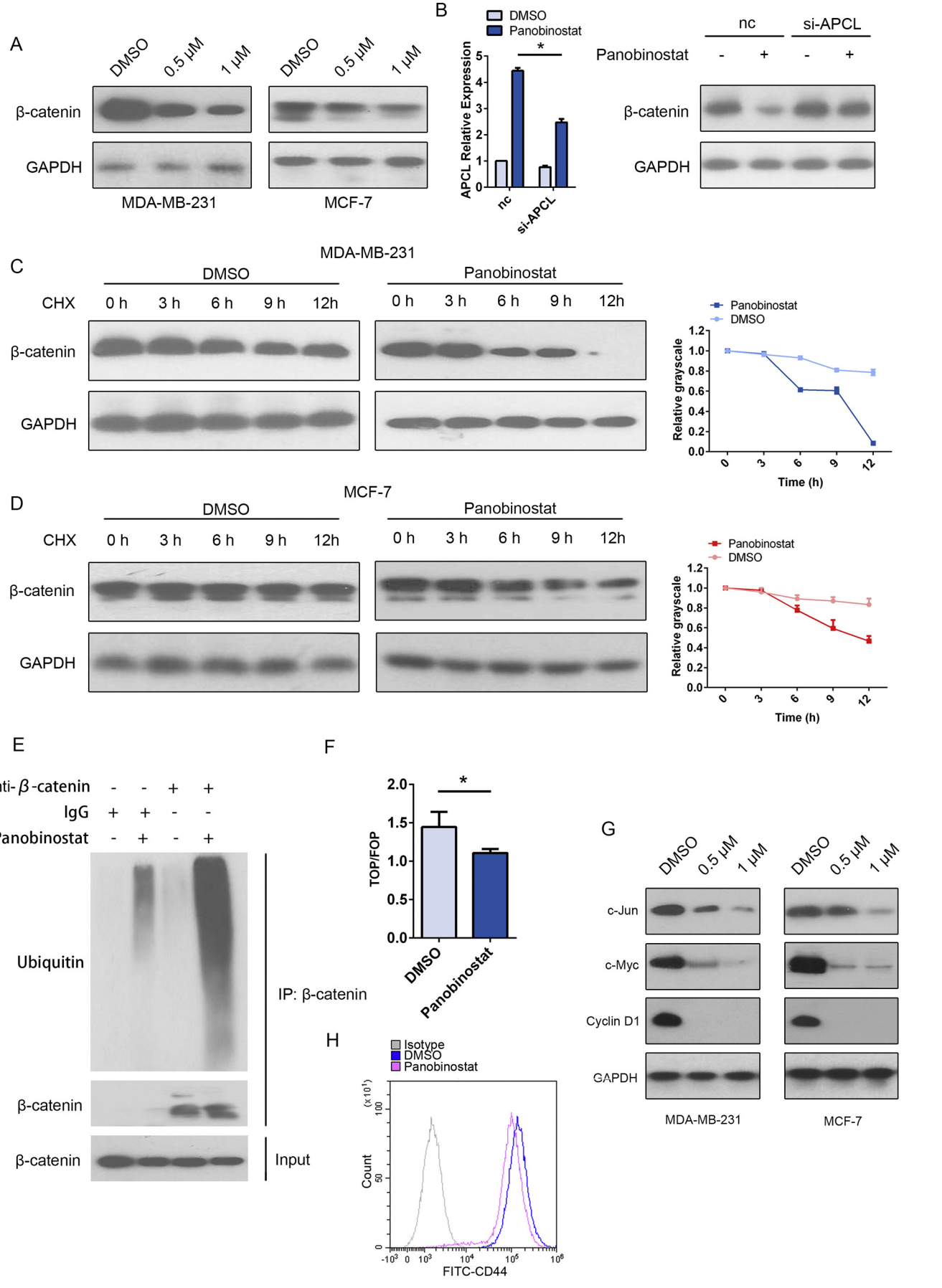

(caption on next page)

Fig. 6. Panobinostat reduced β-catenin stability and inhibited wnt/β-catenin pathway by inducing APCL expression. (A) β-catenin expression was tested by western blot in MDA-MB-231 and MCF-7 cells with 0 μM, 0.5 μM and 1 μM panobinostat treatment. (B) The expression of APCL was knocked down by si-RNA in MDA-MB-231 cells (left), and β-catenin expression was tested by western blot (right). (C,D) The half-life of β-catenin was detected in MDA-MB-231 and MCF-7 cells. (E) β-catenin was precipitated by its specific antibody, and its ubiquitination was examined with ubiquitin antibody by western blot. (F) TOP Flash and FOP Flash reporter plasmids were transfected in MDA-MB-231 cells and tested by dual-luciferase assay. The result was shown in the form of TOP/FOP. (G) Western blot for c-Jun, c-Myc and Cyclin D1. (H) CD44 expression on the surface of MDA-MB-231 cells treated with 0 μM and 0.5 μM panobinostat was analyzed by flow cytometry. Data were presented as mean ± s.d. of three independent experiments, and the significance of difference between groups was analyzed by Student's *t*-test. $^{*}P < .05$.

panobinostat significantly suppressed β-catenin protein expression (Fig. 6A), which was rescued by the knockdown of APCL (Fig. 6B).

Next, cycloheximide (CHX) was added to cells to evaluate the half-time of β-catenin. As shown in Fig. 6C and D, panobinostat promoted β-catenin dagration and led to a shorter half-life in both MDA-MB-231 and MCF-7 cells. Consistently, co-IP assay showed the ubiquitination of β-catenin was increased by 1 μM panobinostat (Fig. 6E).

In addition, we examined the downstream effectors of β-catenin. TOP/FOP flash assay was conducted to evaluate β-catenin mediated transcriptional activity. It revealed that β-catenin induced gene transcription was reduced by 0.5 μM panobinostat (Fig. 6F). The expression of the β-catenin target genes were also tested by western blot, and c-Jun, c-Myc, Cyclin D1 and TEF were decreased by panobinostat in a concentration dependent manner (Fig. 6G). CD44 was also known to be regulated by β-catenin, and as MDA-MB-231 cells had relative higher expression of CD44, we detected its surface CD44 expression by FACS analysis. As shown in Fig. 6H, cell surface CD44 expression was inhibited by 0.5 μM panobinostat.

These results suggested that panobinostat reduced β-catenin stability and inhibited wnt/β-catenin pathway by inducing APCL expression.

3.7. Panobinostat inhibited the growth and metastasis of breast cancer xenografts

An *in vivo* study was conducted to further evaluate the anti-tumor effect of panobinostat. 2×10^6 MDA-MB-231 cells were subcutaneously injected into female nude mice ($n = 8$/group). One week late, 20 mg/kg panobinostat was intraperitoneally injected in nude mice three times a week, and the tumor volume was measured once a week. The result showed that the tumor volume of the panobinostat treated group was significantly smaller (Fig. 7A and B). The expression of APCL and β-catenin of tumor xenograft tissues were detected by immumohistochemical staining. As shown in Fig. 6C, APCL expression was upregulated in panobinostat treated mice while it was barely detectable in the control group. Consistently, β-catenin expression was downregulated in the panobinostat treated group.

Moreover, lung metastasis animal model was generated through tail vein injection with MDA-MB-231 cells stably transfected with luciferase. Bioluminescence imaging (BLI) was applied to visualize lung metastases, and the mice were imaged once every week starting 4 weeks after cell injection. The final BLI data showed that the signal in untreated mice was substantially stronger than that in panobinostat-treated mice using the same BLI parameters (Fig. 7D). BLI signal was also quantified by IVIS system and analyzed in log scale (Fig. 7E). These data indicated that the tumor burden was alleviated by panobinostat. Lungs were excised and HE staining was performed to confirm pathological metastasis in the lungs. Some tiny metastasis nodules not detected by BLI were found under microscope, and the total numbers of metastatic tumors were counted. The result showed that pulmonary metastasis rate was 6/6 in vehicle-treated mice, while that in panobinostate-treated mice was 4/6 (Fig. S1B). IHC staining was also used to detect APCL and β-catenin expression in lung metastatic tumors. Consistently, APCL expression was upregulated in panobinostat treated group while β-catenin expression was decreased by panobinostat treatment (Fig. 7F).

4. Discussion

Breast cancer is the most common malignant disease in women worldwide. In this study, we evaluated the anti-tumor effect of a novel compound, panobinostat, in breast cancer cells of different subtypes. Furthermore, we demonstrated that the tumor suppressor gene APCL was a crucial target of panobinostat. The compound exerted its breast cancer inhibition activity by upregulating APCL transcription and consequently reduced the activity of its downstream wnt/β-catenin signaling pathway.

Panobinostat is a pan-HDAC inhibitor and is reported to have therapeutic effect in multiple malignant diseases like lung cancer [20], multiple myeloma [21], glioblastoma [22], acute lymphoblastic leukaemia [23] and breast cancer [24]. Tate et al. had reported panobinostat inhibited the proliferation of triple-negative breast cancer cells [12], which was in accordance with our findings. So far, most of the studies on panobinostat have focused on TNBC. Here we showed that panobinostat had anti-tumor effect on both TNBC and non-TNBC cells by inhibiting cell proliferation, clone formation and inducing apoptosis. The inhibitory activity of panobinostat on metastasis was also demonstrated in this study *in vitro* and *in vivo*. Panobinostat suppressed the migration and invision of both TNBC and non-TNBC cells. Though the ZEB family of transcription factors were reported to be suppressed by panobinostat in TNBC[13], we found other important EMT makers like vimentin and slug were also downregulated by panobinostat.

The mechanism of panobinostat in cancer treatment remains elusive. Yao et al. revealed panobinostat inhibited glioblastoma growth by suppressing HIF-1α expression [25]. Another oncogene, FOS-like antigen 1, was also reported to be a molecular target of panobinostat, and the compound induced apoptosis and G2/M cell cycle arrest in undifferentiated pleomorphic sarcoma *via* inhibiting FOS-like antigen 1 [26]. Besides, Song et al. demonstrated that panobinostat inhibited proliferation and metastasis of hepatocellular carcinoma *via* suppression of the gankyrin/stat3/Akt pathway [27]. Accumulating studies have indicated that histone acetylation plays an important role in gene transcription regulation. The high level of acetylated histones loosens the chromatin conformation and facilitates the binding of transcription factors to the promoter regions of many genes. Panobinostat effectively increases histone acetylation *via* inhibiting multiple HDACs, which results in enhanced gene transcription in most cases. Therefore, we speculated that the transcription of certain tumor suppressor genes might be increased by panobinostat, and used RNA microarray assay to search for candidate genes upregulated after panobinostat treatment.

One of these genes, APCL, encoded a protein closely related to the adenomatous polyposis coli (APC) protein and had similar tumor suppressor function. APCL was first identified as a brain-specific APC homologue, but subsequently found in malignant tumors [14,16]. In our study, we found APCL was almost undetectable in breast cancer cells, but its expression had a several-fold increase after panobinostat treatment. Consistently, its promoter activity was also upregutated by panobinostat. When APCL was knocked down, the anti-proliferation activity of panobinostat was reduced in breast cancer cells. Moreover, we analyzed the prognostic value of APCL using Kaplan-Meier Plotter. The survival analysis showed that patients with APCL high expression had better outcomes in the whole cohort, luminal A subtype, lunminal B subtype and tripe-negative breast cancer patients. In contrast, it had no statistical significance in the HER-2 amplified cohort. This result was

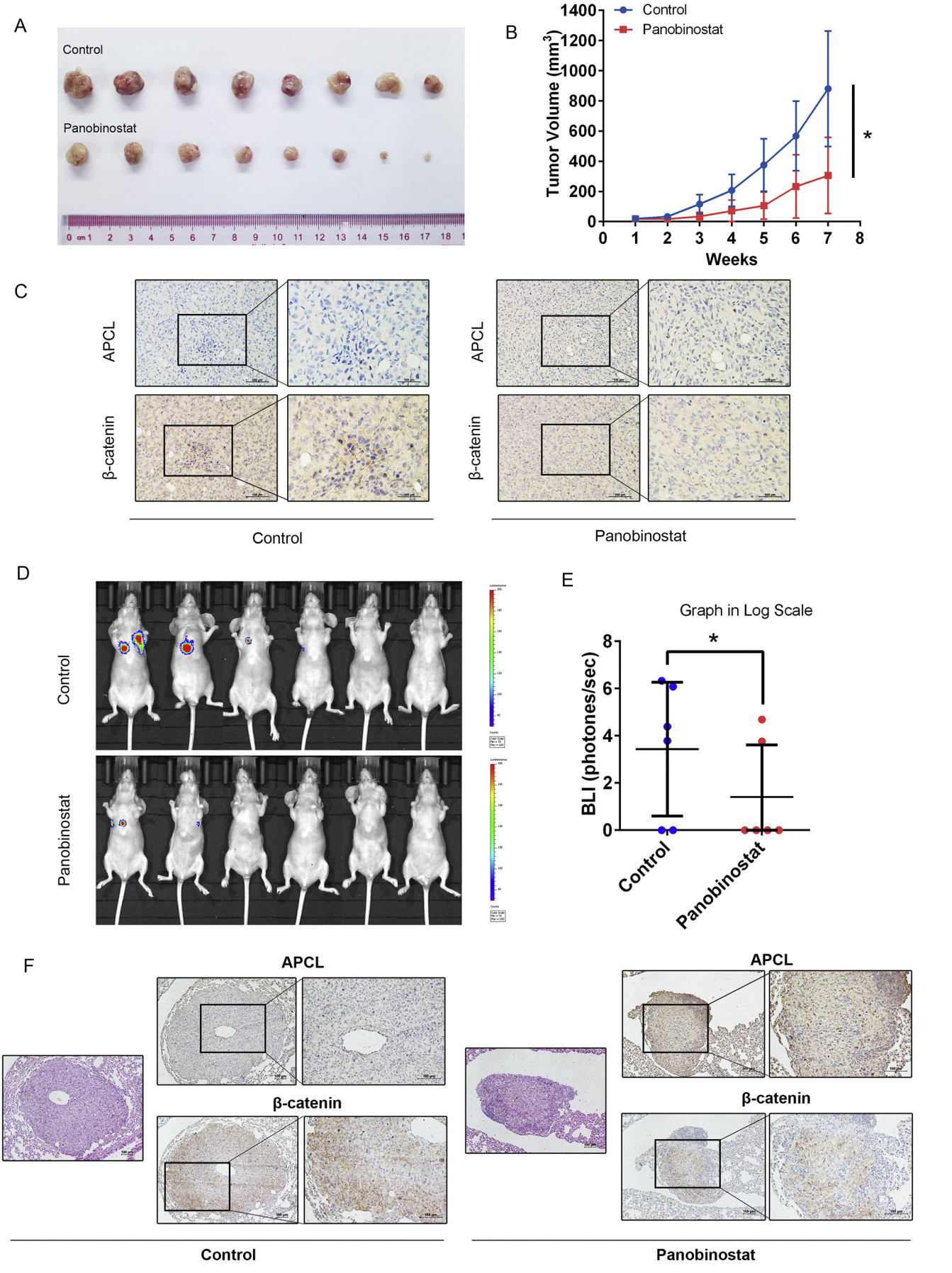

(caption on next page)

Fig. 7. Panobinostat inhibited breast cancer growth and metastasis *in vivo*. (A) Tumor xenografts from control and panobinostat-treated mice were excised in the seventh week after cell injection. (B) The tumor volumes of control and panobinostat-treated mice were recorded and analyzed weekly. (C) The expression of APCL and β-catenin were detected by immuohistochemical staining in tumor tissues. (D) Bioluminescence images of mice with MDA-MB-231-LUC trail vein injection. (E) BLI value was quantified and presented in log scale. (F) IHC staining of APCL and β-catenin in lung metastatic tumors. Data were presented as mean ± s.d, and the significance of difference between groups was analyzed by Student's *t*-test. $^{*}P < .05$.

consistent with our MTS data, in which the HER-2 amplified cell line SKBR3 was resistant to panobinostat. Our results suggested that panobinostat promoted APCL transcription and expression to exert its anti-tumor effect in breast cancer cells.

Next, we tried to further validate the downstream functions of APCL. Similar to APC, APCL is a wnt/β-catenin pathway regulator. APCL interacted with Axin and constituted the β-catenin destruction complex [28]. As has been proved by several researches, this complex accelerated β-catenin ubiquitination and its subsequent degradation by proteasome [29,30]. β-catenin is a powerful oncogene and highly expressed in many kinds of malignant diseases. The multiple functions of β-catenin include promoting cell proliferation, epithelial-mesenchymal transition (EMT) and preventing apoptosis [31,32]. Ying et al. revealed MiR-939 promoted the proliferation of human ovarian cancer cells by repressing APCL and upregulating β-catenin expression [33]. In our research, the protein level of β-catenin was reduced by panobinostat treatment but was reversed by APCL knockdown. In addition, we found that panobinostat caused increased ubiquitination and degradation of β-catenin, and accordingly the inhibition of its target oncogenes such as c-Jun, c-Myc, CD44 and Cyclin D1 [34–36].

5. Conclusions

In summary, we conclude that panobinostat exerted anti-tumor effect in both TNBC and non-TNBC cells *via* the APCL/β-catenin pathway. Our pre-clinical study suggests that APCL is a crucial target of panobinostat in breast cancer treatment. Given that panobinostat has a low selectivity in HDACs inhibition, it needs further investigation to identify the exact HDAC(s) that regulates APCL transcription, which may lead to the development of HDAC inhibitors with better specificity.

Ethics approval and consent to participate

Animal care and experiments involved in this study were consistent with Accreditation of Laboratory Animal Care International guidelines. Animals and protocols were approved by the guidelines established by the Animal Care Committee at Sun Yat-sen University.

Availability of data and material

The database analyzed during the current study are available in the Kaplan-Meier Plotter (http://kmplot.com/analysis). Other data supporting the findings of this study are available within the article.

Competing interests

The authors have no conflicts of interest to declare.

Funding

This work was supported by the funds from the National Natural Science Foundation of China (81472178, 81772925, 81702761), the Natural Science Foundation of Guangdong (2017A030313615, 2016A030311002), and Guangzhou Science Technology and Innovation Commission (201607020038).

Authors' contributions

Conception and design: Ge Qin, Wuguo Deng.

Development of methodology: Ge Qin, Xin Wang, Yizhuo Li.

Acquisition of data: Ge Qin, Yanlai Tang, Dingbo Shi.

Analysis and interpretation of data: Ge Qin, Kai Zhang, Kaping Li, Huijuan Qiu.

Writing, review, and/or revision of the manuscript: Ge Qin, Miao Chen, Wuguo Deng, Xiangdong Xu.

Administrative, technical, or material support: Changlin Zhang, Qian Long, Qinglian Zhai, Shusen Wang.

All authors read and approved the final manuscript for publication.

Supplementary data to this article can be found online at https://doi.org/10.1016/j.cellsig.2019.03.014.

Acknowledgements

We are grateful to Novartis for the panobinostat compound. We thank our colleagues for their helpful discussions.

References

[1] L.A. Torre, F. Islami, R.L. Siegel, E.M. Ward, A. Jemal, Global cancer in women: burden and trends, Cancer Epidemiol. Biomark. Prev. 26 (2017) 444–457.
[2] S. Khorasanizadeh, The nucleosome: from genomic organization to genomic regulation, Cell 116 (2004) 259–272.
[3] V.G. Allfrey, R. Faulkner, A.E. Mirsky, Acetylation and methylation of histones and their possible role in the regulation of RNA synthesis, Proc. Natl. Acad. Sci. U. S. A. 51 (1964) 786–794.
[4] M. Haberland, R.L. Montgomery, E.N. Olson, The many roles of histone deacetylases in development and physiology: implications for disease and therapy, Nat. Rev. Genet. 10 (2009) 32–42.
[5] A.J. Bannister, T. Kouzarides, Regulation of chromatin by histone modifications, Cell Res. 21 (2011) 381–395.
[6] E. Seto, M. Yoshida, Erasers of histone acetylation: the histone deacetylase enzymes, Cold Spring Harb. Perspect. Biol. 6 (2014) a018713.
[7] M.F. Fraga, E. Ballestar, A. Villar-Garea, et al., Loss of acetylation at Lys16 and trimethylation at Lys20 of histone H4 is a common hallmark of human cancer, Nat. Genet. 37 (2005) 391–400.
[8] S. Karsli-Ceppioglu, A. Dagdemir, G. Judes, et al., Epigenetic mechanisms of breast cancer: an update of the current knowledge, Epigenomics 6 (2014) 651–664.
[9] X. Li, J. Zhang, Y. Xie, Y. Jiang, Z. Yingjie, W. Xu, Progress of HDAC inhibitor panobinostat in the treatment of cancer, Curr. Drug Targets 15 (2014) 622–634.
[10] Q. Zhou, P. Atadja, N.E. Davidson, Histone deacetylase inhibitor LBH589 reactivates silenced estrogen receptor alpha (ER) gene expression without loss of DNA hypermethylation, Cancer Biol. Ther. 6 (2007) 64–69.
[11] M. Kubo, N. Kanaya, K. Petrossian, et al., Inhibition of the proliferation of acquired aromatase inhibitor-resistant breast cancer cells by histone deacetylase inhibitor LBH589 (panobinostat), Breast Cancer Res. Treat. 137 (2013) 93–107.
[12] C.R. Tate, L.V. Rhodes, H.C. Segar, et al., Targeting triple-negative breast cancer cells with the histone deacetylase inhibitor panobinostat, Breast Cancer Res. 14 (2012) R79.
[13] L.V. Rhodes, C.R. Tate, H.C. Segar, et al., Suppression of triple-negative breast cancer metastasis by pan-DAC inhibitor panobinostat via inhibition of ZEB family of EMT master regulators, Breast Cancer Res. Treat. 145 (2014) 593–604.
[14] H. Nakagawa, Y. Murata, K. Koyama, et al., Identification of a brain-specific APC homologue, APCL, and its interaction with beta-catenin, Cancer Res. 58 (1998) 5176–5181.
[15] S. Munemitsu, I. Albert, B. Souza, B. Rubinfeld, P. Polakis, Regulation of intracellular beta-catenin levels by the adenomatous polyposis coli (APC) tumor-suppressor protein, Proc. Natl. Acad. Sci. U. S. A. 92 (1995) 3046–3050.
[16] C.S. Daly, P. Shaw, L.D. Ordonez, et al., Functional redundancy between Apc and Apc2 regulates tissue homeostasis and prevents tumorigenesis in murine mammary epithelium, Oncogene. 36 (2017) 1793–1803.
[17] M.G. Catalano, M. Pugliese, E. Gargantini, et al., Cytotoxic activity of the histone deacetylase inhibitor panobinostat (LBH589) in anaplastic thyroid cancer in vitro and in vivo, Int. J. Cancer 130 (2012) 694–704.
[18] M.C. Crisanti, A.F. Wallace, V. Kapoor, et al., The HDAC inhibitor panobinostat (LBH589) inhibits mesothelioma and lung cancer cells in vitro and in vivo with particular efficacy for small cell lung cancer, Mol. Cancer Ther. 8 (2009) 2221–2231.
[19] A. Lanczky, A. Nagy, G. Bottai, et al., miRpower: a web-tool to validate survival-associated miRNAs utilizing expression data from 2178 breast cancer patients, Breast Cancer Res. Treat. 160 (2016) 439–446.
[20] A. Edwards, J. Li, P. Atadja, K. Bhalla, E.B. Haura, Effect of the histone deacetylase

inhibitor LBH589 against epidermal growth factor receptor-dependent human lung cancer cells, Mol. Cancer Ther. 6 (2007) 2515–2524.
[21] H. Bailey, D.D. Stenehjem, S. Sharma, Panobinostat for the treatment of multiple myeloma: the evidence to date, J. Blood Med. 6 (2015) 269–276.
[22] L.M. Pont, K. Naipal, J.J. Kloezeman, et al., DNA damage response and anti-apoptotic proteins predict radiosensitization efficacy of HDAC inhibitors SAHA and LBH589 in patient-derived glioblastoma cells, Cancer Lett. 356 (2015) 525–535.
[23] P. Garrido Castro, E.H.J. van Roon, S.S. Pinhancos, et al., The HDAC inhibitor panobinostat (LBH589) exerts in vivo anti-leukaemic activity against MLL-rearranged acute lymphoblastic leukaemia and involves the RNF20/RNF40/WAC-H2B ubiquitination axis, Leukemia. 32 (2018) 323–331.
[24] P. Fedele, L. Orlando, S. Cinieri, Targeting triple negative breast cancer with histone deacetylase inhibitors, Expert Opin. Investig. Drugs 26 (2017) 1199–1206.
[25] Z.G. Yao, W.H. Li, F. Hua, et al., LBH589 inhibits glioblastoma growth and angiogenesis through suppression of HIF-1alpha expression, J. Neuropathol. Exp. Neurol. 76 (2017) 1000–1007.
[26] Y. Saitoh, C. Bureta, H. Sasaki, et al., The histone deacetylase inhibitor LBH589 inhibits undifferentiated pleomorphic sarcoma growth via downregulation of FOS-like antigen 1, Mol. Carcinog. 58 (2) (2018) 234–246.
[27] X. Song, J. Wang, T. Zheng, et al., LBH589 inhibits proliferation and metastasis of hepatocellular carcinoma via inhibition of gankyrin/STAT3/Akt pathway, Mol. Cancer 12 (2013) 114.
[28] H.E. Croy, C.N. Fuller, J. Giannotti, et al., The poly(ADP-ribose) polymerase enzyme Tankyrase antagonizes activity of the beta-catenin destruction complex through ADP-ribosylation of Axin and APC2, J. Biol. Chem. 291 (2016) 12747–12760.
[29] S. Dokanehiifard, B.M. Soltani, Hsa-miR-11181 regulates Wnt signaling pathway through targeting of APC2 transcripts in SW480 cell line, Gene. 641 (2018) 297–302.
[30] M.A. Young, C.S. Daly, E. Taylor, R. James, A.R. Clarke, K.R. Reed, Subtle deregulation of the Wnt-signaling pathway through loss of Apc2 reduces the fitness of intestinal stem cells, Stem Cells 36 (2018) 114–122.
[31] R. Kumar, M.D. Bashyam, Multiple oncogenic roles of nuclear beta-catenin, J. Biosci. 42 (2017) 695–707.
[32] J. Liu, C. Huang, C. Peng, et al., Stromal fibroblast activation protein alpha promotes gastric cancer progression via epithelial-mesenchymal transition through Wnt/ beta-catenin pathway, BMC Cancer 18 (2018) 1099.
[33] Y. Xiong, L.Y. Qi, F. Zhou, Y. Wang, J.H. Liu, MiR-939 promotes the proliferation of human ovarian cancer cells by repressing APC2 expression, Biomed. Pharmacother. 71 (2015) 64–69.
[34] J. Xu, Y. Chen, D. Huo, et al., Beta-catenin regulates c-Myc and CDKN1A expression in breast cancer cells, Mol. Carcinog. 55 (2016) 431–439.
[35] C. Trierweiler, H.E. Blum, P. Hasselblatt, The transcription factor c-Jun protects against liver damage following activated beta-catenin signaling, PLoS One 7 (2012) e40638.
[36] B. Taciak, I. Pruszynska, L. Kiraga, M. Bialasek, M. Krol, Wnt signaling pathway in development and cancer, J. Physiol. Pharmacol. 69 (2018).